

Quark States near a Threshold and the Unstable H -dibaryon*

S. V. Bashinsky and R. L. Jaffe

*Center for Theoretical Physics
Laboratory for Nuclear Science
and Department of Physics
Massachusetts Institute of Technology
Cambridge, Massachusetts 02139*

(MIT-CTP-2643, hep-ph/9705407. May 1997)

Abstract

We consider the interplay of a quark state and a hadronic threshold in the framework of the P -matrix formalism, which is reviewed and extended for use together with conventional methods of computing quark-gluon dynamics. We provide a quantitative dynamical interpretation of the reduced R or K matrices and their poles that suggests a natural classification of threshold phenomena. At a threshold with a quark state close to it up to three S -matrix poles can be found. The scattering amplitudes for the corresponding cases are discussed. Our analysis is applied to make an outlook for experimental observation of the doubly strange H -dibaryon if it is not stable to strong decays.

*This work is supported in part by funds provided by the U.S. Department of Energy (D.O.E.) under cooperative research agreement #DF-FC02-94ER40818.

I. INTRODUCTION AND SUMMARY

A resonance shape can be dramatically distorted if one of its decay channels has a threshold within the resonance width. A tiny variation of coupling strength may lead to a wide spectrum of physical phenomena such as a slightly bound or a virtual state, a “shoulder”, or a resonance. All these effects are of kinematic origin. We will show that the underlying quark-gluon dynamics can be isolated and quantitatively estimated in a smooth way which is unaffected by such kinematic cataclysms.

There is little doubt that far from threshold singularities, narrow and dramatic effects in scattering amplitudes are to be identified with quasi-stable states of QCD. Little sophistication is required to connect the $\rho(770)$ with $\bar{u}u-\bar{d}d$ or the $\phi(1020)$ with $\bar{s}s$. However, great care must be used when attempting to assign a fundamental QCD interpretation to broad effects like most of those seen in meson-meson scattering above 1 GeV or to striking effects like the $f_0(980)$ and $a_0(980)$ that lie near thresholds (in this case $K\bar{K}$). Identification of many objects of great interest — exotics, hybrids, glueballs, quasi-molecular states, *etc.* — requires us to relate low energy scattering consistently to microscopic quark-gluon dynamics.

We study hadron-hadron scattering at small kinetic energy, where non-relativistic methods suffice. This is an old problem, but there is no general agreement on how to associate quark-gluon “states” with effects seen in low energy scattering. One of the most popular phenomenological tools is the K -matrix parameterization^[1] and its pole analysis. The K -matrix emerges naturally when the interaction is localized at distances small with respect to the de Broglie wavelength of the scattered particles. For a single channel and an energy close enough to the threshold, the conditions for a K -matrix analysis might seem to be met. However, in the real world hadron-hadron systems with small relative momentum are often strongly coupled to other open or closed channels where the wavelength does not exceed the range of interaction. In this case results obtained from solving microscopic quark dynamics must not be directly associated with the many-channel K -matrix. In place of the K -matrix, we will argue that the P -matrix formalism^[2] is more suitable for this purpose. We will also show that the *reduced* K -matrix does allow certain dynamical interpretation.

The theoretical part of our paper, Sections 2 and 3, consists of two general divisions. Sec. 2 is concerned with micro-dynamics on the hadron-size scale and the P -matrix formalism. The following Sec. 3 deals with observable objects such as S -matrix and cross-sections. Some of the results and the organization of these sections are outlined in the rest of the introduction. In Section 4 we discuss the phenomenological implications of our work for the search for a doubly strange H -dibaryon if this six-quark state is not bound.

In Section 2a we review and extend the P -matrix formalism. P is defined, similar to K , as an algebraic transform of the S -matrix but it involves an additional parameter b :

$$P(\varepsilon, b) = i \sqrt{k} \frac{e^{ikb} S(\varepsilon) e^{ikb} + 1}{e^{ikb} S(\varepsilon) e^{ikb} - 1} \sqrt{k}, \quad (1)$$

where we consider a multichannel s -wave with the total energy ε . If for relative distance $r > b$ the hadrons do not interact or the interaction is simple enough to be described with a potential, the P -matrix generalizes the logarithmic derivative of the wave function at $r=b$ (see Section 2a for details). Then P is fully determined by the dynamics in the inner domain $r < b$. The poles of $P(\varepsilon, b)$, or *primitives*, play an important role. Their positions and residues are related to the spectrum of a system confined in a hypothetical spherical shell with a radius depending on b . Such boundary conditions are used in the bag model and could be simulated on a lattice. In Section 2b we illustrate the P -matrix calculation taking the bag model as an example. The issue of flavor symmetry is addressed. We show that $P_{ij}(\varepsilon, b)$ reflects this symmetry provided the shell is sufficiently small. Then the flavor projection of the quark-bag states onto a two-hadron state determines the corresponding projection of the P -pole residues.

In Section 3a we reconstruct the S -matrix from the P -matrix and see that a pole in $P(\varepsilon)$ gives a resonance-like term in S . Given an arbitrary background scattering, $\overline{S}(\varepsilon)$, the S -matrix will be written as

$$S_{ij} = \overline{S}_{ij} - i \chi_i \frac{1}{\varepsilon - \varepsilon_r + i \frac{\gamma}{2}} \chi_j. \quad (2)$$

where $\chi_i(\varepsilon)$, $\varepsilon_r(\varepsilon)$, and $\gamma(\varepsilon)$ are specified by $\overline{S}(\varepsilon)$ and the P -matrix poles. The unitarity of the S -matrix is preserved automatically. For a narrow P pole eq. (2) is, in fact, a Breit-Wigner resonance but in general the energy dependence in χ_i , ε_r , and γ allows a broad spectrum of physical phenomena. We discuss those that arise when a pole in $P(\varepsilon)$ (a primitive) occurs near a hadronic threshold in the following Section 3b. We start from a review of the analytical structure of the many-channel S -matrix at a threshold. It will be shown that the pole in P -matrix close to the threshold gives rise to up to *two* poles in $S(\varepsilon)$ that influence the scattering and another, in general *third*, pole may appear in the S -matrix due to potential, or background, scattering. After these preliminaries we consider the inverse logarithmic derivative of the two-hadron wave function at $r=b$ in the channel with the threshold. This quantity is named as the reduced R -matrix, $R^{(red)}$, after Wigner and Eisenbud and is approximately equal to the reduced K -matrix close to the threshold. We obtain a formula for $R^{(red)}$ that will appear to have a transparent dynamical interpretation in which the quark state corresponds to the pole in $R^{(red)}(\varepsilon)$ while the potential scattering specifies its regular

part. This result to some degree justifies the interpretation of the poles in the K -matrix as manifestations of narrow quark states.¹ With the formalism developed we classify the possible threshold effects and consider scattering amplitudes and cross-sections for the corresponding cases. Many of them are illustrated by existing physical systems.

In the Section 4 the previous results are used to explore the experimental manifestations of an unbound six-quark H -dibaryon. In the Appendix we estimate parameters giving the width of this state and the hadronic shift in the H mass due to the influence of open channels.

II. THE P-MATRIX

This method of analyzing two-body reactions was proposed by Jaffe and Low in 1979 in order to test the spectroscopic predictions of quark models especially as they relate to exotic (*e.g.* multi-quark) states. The formalism was initially developed in the context of the bag model, where quarks are confined by a scalar vacuum pressure. However, it applies to any model in which quark and gluon eigenstates are studied without considering their coupling to decay channels. First, we briefly review this formalism and also present new arguments that give a further insight into the connection between low-energy scattering and quark model speculations. In the next subsection we quantitatively estimate the parameters of the P -matrix from the quark-bag model for various two-hadron systems.

A. Formalism

At low kinetic energies hadron-hadron scattering may be described by non-relativistic kinematics. Restricting our attention to zero total spin and zero angular momentum, $S=L=0$, we factor out the center-of-mass motion and consider the wave function of an n -channel two-hadron system in the relative coordinate r . For a given value of a spatial parameter b , a definite energy ε , and r greater than the interaction radius, the most general form of the wave function is

$$\psi_i(r_i) = \sum_{j=1}^n \left\{ \cos[k_i(r_i - b)] \delta_{ij} + \frac{\sin[k_i(r_i - b)]}{k_i} P_{ij} \right\} A_j, \quad (3)$$

¹ Let us emphasize that this interpretation is possible only for the *reduced* K or R matrices and looks controversial at first glance since a pole in $K^{(red)}$ or $R^{(red)}$ occurs when the derivative of the hadron wave function vanishes, $\psi'(r)=0$, while the boundary conditions for the quark-bag states are just the opposite: $\psi(r)=0$.

where $i = 1, \dots, n$ labels the channel and the $\{A_j\}$ are some amplitudes.

The matrix P_{ij} generalizes the logarithmic derivative of $\psi(r)$ for the case of many channels. Comparing eq. (3) to the usual S -matrix parameterization of the scattering wave function and assuming that the reduced two-hadron masses, m , are almost the same in all n channels, we find that P and S -matrices are simply related as ^[2]:

$$S = e^{-ikb} \frac{\frac{1}{\sqrt{k}} P \frac{1}{\sqrt{k}} + i}{\frac{1}{\sqrt{k}} P \frac{1}{\sqrt{k}} - i} e^{-ikb} . \quad (4)$$

After this matrix equation is resolved with respect to P , one arrives at eq. (1). The unitarity of S requires the P -matrix to be hermitian². If the interaction is time reversal invariant, then P is also real. P depends on b according to the equation ^[2]

$$\frac{\partial P}{\partial b} = -P^2 - k^2 . \quad (5)$$

For the present we treat b as a free parameter. Suppose for a moment that the value of b is large enough so that there is no interaction between hadrons for $r \geq b$. If for the energy $\varepsilon = \varepsilon_p(b)$ and some choice of the amplitudes A_j in eq. (3) the normalized wave function of the relative motion vanishes at $r=b$ in all channels, then the P -matrix has a pole at $\varepsilon_p(b)$. As shown in Ref. [2], its residue can be factorized:

$$P_{ij}(\varepsilon) = \bar{P}_{ij}(\varepsilon) + \xi_i \frac{r}{\varepsilon - \varepsilon_p} \xi_j^T . \quad (6)$$

We choose the vector ξ to be normalized: $\sum_{i=1}^n \xi_i^2 = 1$. Obviously, the converse statement is also valid: if at some energy ε_p the P -matrix has a pole then one can find the amplitudes A_j in eq. (3) such that

$$\frac{\psi_i(b)}{\|\psi\|} = 0 \quad \forall i = 1, \dots, n . \quad (7)$$

Now we are ready to explore the connection between the poles of the P -matrix and the quark-bag calculations. Remember that for now b is taken to be larger than the range of the strong forces. In this case we just saw that the P -matrix poles (primitives) $\varepsilon_p(b)$ occur at the energies at which the relative wave function of the two hadron system vanishes at $r = b$. We claim that these are just the eigenenergies, $\varepsilon_n(R)$, of the multi-quark system that has the quantum numbers of the two-hadron

² At the energy when only the first $m < n$ channels are open, only the upper-left $m \times m$ sub-matrix of S_{ij} is unitary. Nevertheless, the whole $n \times n$ P -matrix is hermitian for all energies.

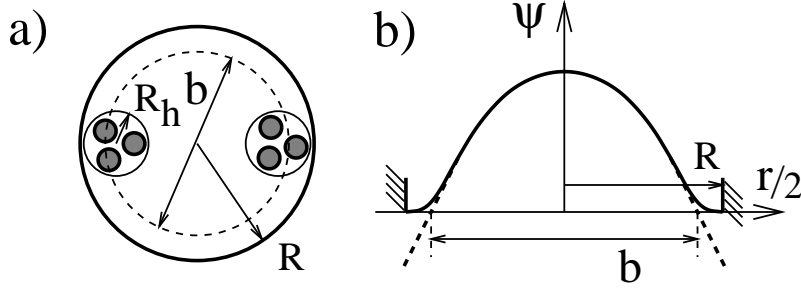


FIG. 1. (a) A two-baryon system is confined in a hypothetical spherical shell with a radius R . (b) Consider a state of this system with a definite energy ε_n (the ground energy in the figure). The wave function of the centers of the $3q$ -subsystems (solid line) strictly vanishes at the shell boundary. At the same energy ε_n , the wave function of the baryons that are not constrained by the shell (dashed line) vanishes when their relative separation equals $b = 2R - 2R_h$.

system and is confined in a hypothetical spherical shell³ with a radius $R(b)$. The radius R is approximately half of b . In fact, if we imagine that the hadrons are constrained in their motion so that the matter density, $\rho(\mathbf{r})$, vanishes when $|\mathbf{r} - \mathbf{R}_{cm}| \geq b$, then the wave function of their relative motion $\psi(r)$ vanishes at

$$b = 2R - 2R_h, \quad (8)$$

where R_h plays the role of the hadron radius, as shown in Fig. 1.

We see that for a large value of b there is one-to-one correspondence between the P -matrix poles and the eigenenergies of a physical system which is put into a hard-wall shell. Now let us make b smaller. The P -matrix, as defined by eq. (1), will preserve a pole structure (see eq. (6)) but the parameters ε_p , r , and ξ will change with b . If b goes to b' the related P -pole shifts to ε'_p , satisfying the equation

$$\varepsilon'_p = \varepsilon_p - \xi^T \frac{r}{P(\varepsilon'_p) + k'_p \cot k'_p \Delta b} \xi \quad \text{where} \quad \Delta b = b' - b. \quad (9)$$

The new residue r' and the channel couplings ξ' can be easily expressed in terms of ε'_p .⁴ Taking a small variation of b one gets the differential equations:

³We require that the center of mass of the system always stays at the shell center. To realize it “technically” one can imagine a massless shell.

⁴The application of the identity eq. (30) and some algebra yield: $\xi' r' \xi'^T = R \xi r \xi^T R^T$ with $R(\varepsilon'_p, \Delta b) \equiv \frac{k'_p}{\sin(k'_p \Delta b)} \frac{1}{P(\varepsilon'_p) + k'_p \cot(k'_p \Delta b)}$.

$$\frac{\partial \varepsilon_p}{\partial b} = -r \quad (10)$$

and

$$\frac{\partial}{\partial b} (\xi r \xi^T) = -\xi r \xi^T \bar{P} - \bar{P} \xi r \xi^T \equiv -\{\xi r \xi^T, \bar{P}\}. \quad (11)$$

The last equation can be also presented as

$$\bar{P}_{ij}(\varepsilon, b) \Big|_{\varepsilon=\varepsilon_p} = -\frac{1}{2r} \frac{\partial r}{\partial b} \xi_i \xi_j - \xi_i \frac{\partial \xi_j}{\partial b} - \frac{\partial \xi_i}{\partial b} \xi_j + \bar{\bar{P}}_{ij}(\varepsilon_p, b) \quad (12)$$

where the matrix $\bar{\bar{P}}$ is orthogonal to the vector ξ : $\bar{\bar{P}}_{ij} \xi_j = \xi_j \bar{\bar{P}}_{ji} = 0$.

It was noted by M. Soldate^[3] that decreasing the radius of the shell in Fig. 1 imposes additional constraints on the system inside and, therefore, causes the eigenenergies of its states, $\varepsilon_n(R)$, to grow. By eq. (10), $r > 0$ is a necessary condition to have

$$\frac{\varepsilon'_p - \varepsilon_p}{b' - b} < 0. \quad (13)$$

It is also the sufficient condition if the matrix $\partial \bar{P}(\varepsilon)/\partial \varepsilon$ is negative semidefinite, in particular if $\bar{P}(\varepsilon)$ is a constant, that can be shown from eq. (9).

When the shell radius reaches the size of a few Fermis we should treat the system inside as a single quark-bag rather than two hadrons, but strong interaction invalidates eq. (3) at such distances. Then it becomes difficult^[4] to relate the system eigenenergies, ε_n , to the position of the P poles, ε_p . Nevertheless, we might expect that there is a size of the shell R_0 when the quark-gluon system inside is already simple enough for our theoretical tools, while $\varepsilon_n(R_0)$ and $\varepsilon_p(b_0)$ are still close to each other. It was proposed in Ref. [2] that at this R_0 the quark system in the shell may be treated as a single bag⁵ and its eigenstates can be calculated in perturbative QCD with current quark masses. This assumption reflects the idea that the bag interior is a phase built up on the perturbative vacuum. Alternatively, it could be a phase in which chiral symmetry is spontaneously broken, yielding constituent quarks with renormalized couplings and pion-like excitations. Finally, one might also attempt to exploit lattice methods. Anyway, if we estimate the position of the P -matrix poles $\varepsilon_p(b_0)$ and their orientation in the channel space $\xi_i(b_0)$, eqs. (10) and (12) will provide us with other ingredients of the P -matrix.

⁵ For a two-nucleon system, *e.g.* deuteron, R_0 must be taken at much larger radius of the pion exchange forces, and this system is better described by the pion exchange potential rather than the quark-bag model.

B. Calculation of P

In principle, *all* the information about the P -matrix can be rigorously obtained from calculations involving only hadronic sizes. To this end one should solve the quark dynamics and parameterize the hadronic wave function according to eq. (3). The external interaction can be taken into account as described in Ref. [2]. In the absence of powerful methods applicable to scales of order 1 fm we resort to bag model phenomenology. To specify $P(\varepsilon)$ we require the primitive energies, ε_p , the residues, $r^{(p)}$, the channel coupling vectors, $\xi_i^{(p)}$, and the nonsingular part, $\overline{P}_{ij}(\varepsilon)$. We treat each of them in sequence below.

The primitive energies were already considered in the previous subsection. Let us remember that they were identified with the eigenenergies, ε_n , of a quark-gluon system subject to confining boundary conditions at a sphere $R(b)$.

In the determination of the vectors $\xi^{(p)}$ it is important to take account of flavor symmetry. For example, one may consider $SU(3)_f$ when describing $\Lambda\Lambda$ scattering or $SU(2)_f$ for the np system. In the scattering of two scalar mesons $SU(3)_f$ is badly violated and the $SU(2)$ isospin symmetry is more appropriate. If the flavor symmetry were exact, the mass of all hadrons belonging to one multiplet would be the same. The states of an interacting system confined by the shell would also form flavor multiplets. The eigenenergies of the states in one multiplet would be equal, and the P -matrix would be $SU(n_f)$ symmetric, whatever the size of the shell. We do not observe this in reality because of the difference in the current quark masses. Nevertheless, the smaller the shell, the better the coupling vector reflects the flavor symmetry. Let us show this in specific examples.

Baryon-Baryon: Imagine two Λ -particles inside a *macroscopic* spherical shell. To be specific, suppose they are in the ground energy state with $J = 0$ and assume that the fusion of the Λ 's into one H -dibaryon ^[5] is energetically forbidden, *i.e.* $M_H > 2M_\Lambda$. For the macroscopic shell the Λ - Λ interaction is negligible, and the ground state is unique with the eigenenergy $\varepsilon_p \simeq 2M_\Lambda$. This $\Lambda\Lambda$ system belongs to the symmetrized product of the two $SU(3)_f$ baryon octets that decomposes into the following irreducible representations:

$$(8 \otimes 8)_{\text{sym}} = 27 \oplus 8 \oplus 1 . \quad (14)$$

However the $\Lambda\Lambda$ state can not be attributed to any of those irreducible parts, therefore the coupling vector ξ_i in the P pole corresponding to the ground state is *not* $SU(3)$ symmetric.

Now we gently contract the shell so that the system remains in its ground state. When the shell radius reaches the order of 1 fm , the scale of the confinement starts to overcome the s -quark mass, and $SU(3)_f$ symmetry gradually emerges. The Λ 's

inside split into a “gas” of 6 strongly interacting quarks. Due to the color-magnetic interaction, the ground state of this system now does occur at the flavor singlet ^{[5], [6]}:⁶

$$|H\rangle = \sqrt{\frac{1}{5}} |BB\rangle + \sqrt{\frac{4}{5}} |\underline{8} \cdot \underline{8}\rangle \quad (15)$$

where $|\underline{8} \cdot \underline{8}\rangle$ denotes a singlet superposition of two color octet baryons and

$$\begin{aligned} |BB\rangle = & \sqrt{\frac{1}{8}} \{ |\Xi^- p\rangle - |\Xi^0 n\rangle + |p \Xi^- \rangle - |n \Xi^0 \rangle \\ & + |\Sigma^- \Sigma^+ \rangle + |\Sigma^+ \Sigma^- \rangle - |\Sigma^0 \Sigma^0 \rangle + |\Lambda \Lambda \rangle \} \end{aligned} \quad (16)$$

is the flavor singlet state composed of two physical baryons.

In order to explore the interpretation of ξ_i as the bag state orientation in the channel space, consider the parameter b in eq. (3) independently for each channel. If at the shell boundary the interaction is negligible, the “partial residue” of the i -th channel will be

$$r\xi_i^2 = -\frac{\partial}{\partial b_i} \varepsilon_p \propto \left. \left| \frac{\partial \psi_i}{\partial r_i} \right|^2 \right|_{r_i=b} \quad (17)$$

(ψ is the normalized wave function of the confined system, obeying $\psi|_{r=b}=0$). Thus $r\xi_i^2$ is associated with the “partial pressure” on the shell walls. Let us consider eq. (17) in the basis where the singlet state given by eq. (16) is one of the basis vectors. Then for a small b we have $\xi_i \simeq \delta_{i,singlet}$, that is the residue $\xi_i r \xi_j^T$ of the lowest P -matrix pole is almost a $SU(3)_f$ singlet. As a first approximation we can take the vector ξ corresponding to the exact $SU(3)_f$ symmetry (*cf.* eq. (16)):

$$\xi_i = \pm \sqrt{\frac{1}{8}}, \quad i = \Xi^- p, \Xi^0 n, p \Xi^-, n \Xi^0, \Sigma^- \Sigma^+, \Sigma^+ \Sigma^-, \Sigma^0 \Sigma^0, \Lambda \Lambda. \quad (18)$$

Meson-Meson: The $f_0(980)$ resonance has the quantum numbers $I(J^{PC}) = 0(0^{++})$ and decays strongly into $\pi\pi$ and $\bar{K}K$. Because of the great difference between the π and K masses, it is not realistic to assume $SU(3)_f$ symmetry even within the confinement radius. The $SU(2)_f$ symmetric decomposition for f_0 reads :

$$\begin{aligned} |f_0\rangle = & \alpha_K \sqrt{\frac{1}{4}} \{ |K^- K^+ \rangle - |\bar{K}^0 K^0 \rangle + |K^+ K^- \rangle - |K^0 \bar{K}^0 \rangle \} + \\ & + \alpha_\pi \sqrt{\frac{1}{3}} \{ |\pi^- \pi^+ \rangle + |\pi^+ \pi^- \rangle - |\pi^0 \pi^0 \rangle \} + \alpha_\eta |\eta\eta\rangle + \alpha_c |c\rangle \end{aligned} \quad (19)$$

⁶Modulo small $SU(3)_f$ violation due to current quark masses.

where $|c\rangle$ stands for confined channels, *e.g.* glueball, and $\sum|\alpha_i|^2 = 1$. Therefore, the P -matrix for $\pi\pi$ scattering has a pole around 980 MeV , and its “orientation” in the channel space ξ is given by the normalized projection of the decomposition (19) onto the two-particle channels $\pi\pi$, $\bar{K}K$, and $\eta\eta$.

Without a deeper understanding of confinement, we are only able to provide crude estimate for the dynamical parameters r and \bar{P} . These will serve as a guide in the next sections. Ref. [2] contains rather visual reasoning concerning the residue r that we paraphrase in the present context as follows. Let us consider the “partial pressure” p_i on the shell walls due to the i -th flavor component of the system:

$$4\pi R^2 p_i \equiv - \frac{\partial \varepsilon_p}{\partial R_i} . \quad (20)$$

We suppose that there is a radius of the shell R_0 when p_i can both be calculated perturbatively in the quark-bag model and attributed to the hadrons in the P -matrix approach. In the two-baryon example above the pressure exerted by the Λ – Λ subsystem is

$$4\pi R^2 p_{\Lambda\Lambda} = - \frac{\partial \varepsilon_n}{\partial R} \lambda \xi_{\Lambda\Lambda}^2 \quad \text{with} \quad \lambda = \frac{1}{5} \quad \text{and} \quad \xi_{\Lambda\Lambda}^2 = \frac{1}{8} , \quad (21)$$

as given by the $SU(3)_f$ symmetric bag model, eqs. (15,16). In the P -matrix formalism it is

$$4\pi R^2 p_{\Lambda\Lambda} = - \frac{\partial b}{\partial R} \frac{\partial \varepsilon_p}{\partial b_{\Lambda\Lambda}} \xi_{\Lambda\Lambda}^2 = \frac{\partial b}{\partial R} r \xi_{\Lambda\Lambda}^2 , \quad (22)$$

see eqs. (17,18). Comparing the right hand sides of eqs. (21) and (22) we get

$$r \simeq \frac{\partial R}{\partial b} \frac{\partial \varepsilon_n}{\partial R} \lambda \Big|_{R=R_0} . \quad (23)$$

The important result is that the residue r is suppressed by the factor $\lambda < 1$ with respect to its natural scale.

If one estimates primitive masses and residues in the bag model, the radius of the confining shell, R_0 , is predetermined by the bag model virial theorem as

$$R_0 \simeq 5M^{1/3} \text{ GeV}^{-1} , \quad (24)$$

where M is the mass of the quark-bag state measured in GeV . In the discussion above we assumed that close to the boundaries of the hypothetical shell in Fig. 1 the quark-gluon matter behaves as two almost non-interacting hadrons. Let these hadrons have comparable masses, $M/2$, and treat them as separate rigid quark bags with the radius given by the formula (24) as

$$R_h \simeq 5 \left(\frac{M}{2} \right)^{1/3} \text{ GeV}^{-1} \simeq \frac{1}{2^{1/3}} R_0 \simeq 0.8 R_0 , \quad (25)$$

so that from eq. (8)

$$b_0 \simeq 2R_0 - 2R_h \simeq 0.4 R_0 . \quad (26)$$

The assumption that the hadrons of the size $2R_h \simeq 1.6R_0$ do not interact in the shell of the diameter $2R_0$ is absurd, and the result (26) should be considered as a lower bound on b_0 . An upper bound can be found from the opposite extreme when the quarks inside the cavity are assumed to be uncorrelated with each other. This was done in the original paper [2] by Jaffe and Low. They chose b_0 that approximately matched the density of the free hadron-hadron wave function, $\psi(r) \propto \sin(\pi r/b_0)$, vanishing at $r = b_0$, to the density of the centers of mass of two-quark clusters (for mesons), when all the quarks in the cavity moved independently. For a meson-meson system that yielded

$$b_0 \simeq 1.4 R_0 , \quad (27)$$

and should give a smaller result for three-quark baryons. From this discussion we conclude that the radius in eq. (24) is too small for reliable calculation of the P -matrix but may suffice for estimates of the order of magnitude, with $b_0 \sim R_0$.

We can say even less about the matrix $\overline{P}(\varepsilon)$. Definitely, it has poles corresponding to the other bag states. Eq. (12) suggests that in the interstitial region

$$\overline{P}_{ij} \sim \frac{1}{b_0} . \quad (28)$$

III. CORRESPONDING S-MATRIX

Now we turn our attention to the quantity connected to actual scattering experiments – the S -matrix. In the Subsection 3a we express S and its singularities in terms of the P -matrix discussed earlier. Then we consider in detail the threshold effects and their interference with primitives.

A. General equations

In the previous section we argued that the poles of the P -matrix have fundamental significance. Taking P in the pole form, eq (6),

$$P_{ij}(\varepsilon) = \overline{P}_{ij}(\varepsilon) + \xi_i \frac{r}{\varepsilon - \varepsilon_p} \xi_j^T , \quad (29)$$

one can easily reconstruct the corresponding S -matrix from eq. (4). In the denominator of eq. (4) one has to deal with the inversion of a matrix having the structure $A_{ij} + \xi_i a \xi_j^T$ and the following identity comes handy

$$\frac{1}{A + \xi a \xi^T} = \frac{1}{A} - \frac{1}{A} \xi \frac{a}{1 + \xi^T \frac{a}{A} \xi} \xi^T \frac{1}{A} . \quad (30)$$

After some calculations we obtain

$$S_{ij} = \bar{S}_{ij} - i \chi_i \frac{1}{\varepsilon - \varepsilon_r + i \frac{\gamma}{2}} \chi_j . \quad (31)$$

In this formula \bar{S} is the background or potential scattering produced by $\bar{P}(\varepsilon)$:

$$\bar{S}(\varepsilon) = e^{-ikb} \frac{\frac{1}{\sqrt{k}} \bar{P} \frac{1}{\sqrt{k}} + i}{\frac{1}{\sqrt{k}} \bar{P} \frac{1}{\sqrt{k}} - i} e^{-ikb} . \quad (32)$$

Eq. (32) also enables one to find $\bar{P}(\varepsilon)$ when the potential scattering, $\bar{S}(\varepsilon)$, is known. The pole term in eq. (31) has diverse manifestations in cross-sections, that are discussed in the next subsection. As shorthand for them we will make free use of the word “resonance” recognizing that a true resonance occurs only under somewhat limited conditions. The “resonance” couplings to the hadronic channels χ_i are

$$\chi_i(\varepsilon) = \sqrt{2r} e^{-ik_i b} \sqrt{k_i} \left(\frac{1}{\bar{P} - ik} \right)_{ij} \xi_j . \quad (33)$$

For the energy dependent “resonance” position and the width in the denominator of eq. (31) we have

$$\varepsilon_r(\varepsilon) - i \frac{\gamma(\varepsilon)}{2} = \varepsilon_p - \xi^T \frac{r}{\bar{P} - ik} \xi . \quad (34)$$

The real and imaginary parts in eq. (34) can be easily separated. In order to do it, we write the many-channel momentum matrix k as

$$k = q + i\kappa , \quad (35)$$

where q and κ are real and refer to the open and closed channels correspondingly. Recalling that for the strong interaction \bar{P} is also real, we find

$$\varepsilon_r(\varepsilon) = \varepsilon_p - \xi^T \frac{r}{\bar{P} + \kappa + q \frac{1}{\bar{P} + \kappa} q} \xi , \quad (36)$$

$$\gamma(\varepsilon) = 2r \xi^T \frac{1}{\sqrt{1 + \left(\frac{1}{\bar{P} + \kappa} q \right)^2}} \frac{1}{\bar{P} + \kappa} q \frac{1}{\bar{P} + \kappa} \frac{1}{\sqrt{1 + \left(q \frac{1}{\bar{P} + \kappa} \right)^2}} \xi . \quad (37)$$

These equations are valid for a nonsingular $\bar{P} + \kappa$ and an arbitrary q . One can write the total width in eq. (37) as a sum of partial width γ_i over only the open channels:

$$\gamma = \sum_{\substack{\text{open} \\ \text{channels}}} \gamma_i \quad (38)$$

with the i -th partial width:

$$\gamma_i = 2rq_i \left(\frac{1}{\overline{P} + \kappa} \frac{1}{\sqrt{1 + \left(q \frac{1}{\overline{P} + \kappa}\right)^2}} \xi \right)_i^2 . \quad (39)$$

As expected, the elements S_{ij} in eq. (31) between the *open* channels form a unitary sub-matrix:

$$S^{(0)} S^{(0)\dagger} = 1 , \quad (40)$$

where $S^{(0)}$ stands for the physical scattering matrix that is the restriction of S to the open channels. Note that the unitarity of the physical S -matrix does not impose any additional restrictions on the P -matrix poles and residues or on the $\overline{S}(\varepsilon)$, except that the physical part of \overline{S} be unitary by itself. As long as P is hermitian, S -matrix unitarity is automatically taken care by eq. (4).

As we saw earlier, $P(\varepsilon, b_0)$ is completely determined by the dynamics in the microscopic domain where the interaction is strong, and it is not influenced by the region in the configuration space where the system is represented by two freely moving hadrons. Thus, *all kinematical effects are absorbed in eqs. (31-37)*. We proceed to study them next.

B. Threshold analysis

At a threshold the kinematics plays a key role. Threshold singularities of the S -matrix and their analytical structure are well known and conveniently described in the K -matrix parameterization. The P -matrix formalism should provide similar results but allows a dynamical point of view, however. In fact, we argue that at a threshold the reduced K -matrix and its poles also have a quantitative *dynamical* interpretation. The object of this section is to give a simple classification scheme for threshold effects and present an account of observed cross-sections for those cases. Let us emphasize that although threshold phenomena by themselves are well investigated, a quark state nearby may produce some deviations from the “standard” picture.

The analytical structure of $S(\varepsilon)$ at a threshold is complicated by its many-sheeted structure with a branch point at the threshold energy. The usual correspondence between S -matrix poles and physical states becomes more subtle. In fact, it is known [7] that two different kind of poles may appear. In Ref. [7] Pennington points out that a bound or a virtual state near a threshold produced by a long-range potential gives rise to only one pole in the S -matrix. On the other hand, a tightly bound multi-quark state results in a pole on each energy sheet, and at a threshold, where two

sheets merge, the two poles are equally important. We incorporate this observation into a general scheme. The S -matrix singularity analysis will provide a systematic arrangement of physical phenomena that to a good extent is independent of specific experimental circumstances.

Suppose the P -matrix has a pole at the energy ε_p in the vicinity of a threshold. It might be the H -dibaryon at $\Lambda\Lambda$ threshold (2230 MeV) or $f_0(980)/a_0(980)$ at $\bar{K}K$ threshold (990 MeV). The S -matrix in eq. (31) has a pole at the energy ε_s when the denominator $\varepsilon - \varepsilon_r(\varepsilon) + i\gamma(\varepsilon)/2$ vanishes. Taking $\varepsilon_r - i\gamma/2$ from eq. (34) we get the following equation for the S poles generated by the quark state:

$$\varepsilon_s = \varepsilon_r(\varepsilon_s) - i \frac{\gamma(\varepsilon_s)}{2} = \varepsilon_p - \xi^T \frac{r}{\bar{P}(\varepsilon_s) - ik(\varepsilon_s)} \xi . \quad (41)$$

The right hand side of eq. (41) is a multivalued function because the momentum

$$k(\varepsilon) = \text{diag}(k_1, \dots, k_n) = \text{diag}\left(\sqrt{2m(\varepsilon - \varepsilon_{\text{th}1})}, \dots, \sqrt{2m(\varepsilon - \varepsilon_{\text{th}n})}\right) \quad (42)$$

has branch points at all threshold energies $\varepsilon_{\text{th}i}$. We will call the channel with its threshold close to the P pole the “singular” one and the other channels, correspondingly, “non-singular”. A pole in $S(\varepsilon)$ disturbs the cross-section if only its position on the complex energy Riemann surface is close enough to the physical region, which is the side of the real energy cut where each k_i is either real and positive (for open channels) or $k_i = i\kappa_i$ with real and positive κ_i (for closed channels). Accordingly, we are interested in the solutions of eq. (41) for which all non-singular channel momenta are taken to be close to the positive real or upper imaginary semi-axis. As for the singular momentum branches, each of them is important provided the corresponding solution of eq. (41) is close enough to the threshold. The natural measure of being “close enough” on the k_{singular} complex plane is $1/b_0$, as will be seen in the course of our work. That is when we reckon only one channel as the singular one at our energy range, we have assumed that in all the other coupled channels the momenta, perhaps imaginary, are larger than $1/b_0$ in absolute value.

Let us suppose that at the threshold under consideration all the non-singular channels are closed and label the singular one with the subscript $i=1$. This condition is applicable to the $\Lambda\Lambda$ threshold in the previous baryon-baryon example or for NN scattering. It is not true for the $f_0(980)$ or $a_0(980)$ resonances near $K\bar{K}$ -threshold because the non-singular $\pi\pi$ channel is open. In the general case, discussed at the end of the section, our equations below remain unchanged but most of the parameters become complex. In the following work we are neglecting the energy dependence in the background term \bar{P} and in the non-singular momenta $k_{i \neq 1}$. As for \bar{P} , it must be a good approximation inside the complex circle

$$|k_1 b_0| < 1 , \quad (43)$$

if we suppose that no other P poles occur in this energy range. The energy interval corresponding to eq. (43) is around 20 MeV for $\Lambda\Lambda$ and 60 MeV for $K\bar{K}$ scattering. In these and many other cases $k_{i \neq 1} \simeq const$ is also valid in the most of the range (43).

Eq. (41) for the S poles energy can be rewritten in terms of the related momentum in the singular channel k_{1s} ($\varepsilon_s = k_{1s}^2/2m + \varepsilon_{th1}$) as

$$\varepsilon_{th1} + \frac{k_{1s}^2}{2m} = \varepsilon_p + \Delta\varepsilon_p - i \frac{k_{1s}\rho_1 c_1/2m}{c_1 - ik_{1s}}, \quad (44)$$

where $\Delta\varepsilon_p$, ρ_1 , and c_1 are the following parameters

$$\Delta\varepsilon_p \equiv -\xi^T \frac{r}{\bar{P} + \bar{\kappa}} \xi, \quad \rho_1 \equiv 2mr \left[\left(\frac{1}{\bar{P} + \bar{\kappa}} \right)_{1i} \xi_i \right]^2, \quad c_1 \equiv \left[\left(\frac{1}{\bar{P} + \bar{\kappa}} \right)_{11} \right]^{-1}, \quad (45)$$

and

$$\bar{\kappa}_l \equiv \begin{cases} \frac{1}{i}k_l, & l \neq 1; \\ 0, & l = 1. \end{cases} \quad (46)$$

Notice that $\bar{\kappa}$ and the parameters in eq. (45) are real since we work with the lowest threshold ($\varepsilon_{th1} < \varepsilon_{th\ l, l \neq 1}$), and they are approximately constants in the circle described by eq. (43) where $\bar{P}, \bar{\kappa} \simeq const$. In this approximation eq. (44) is cubic with respect to the unknown k_{1s} . That is we can find from zero to three S -matrix poles inside the near-threshold circle, eq. (43).

There is a natural physical interpretation for all the three possible solutions of eq. (44) as well as for the parameters defined by eq. (45). First we consider the narrow resonance limit $r \rightarrow 0$ so that $\rho_1 \rightarrow 0$ and $\Delta\varepsilon_p \rightarrow 0$. Then the solutions of eq. (44) are

$$k_{1s}^{(1,2)} \simeq \pm \sqrt{2m(\varepsilon_p - \varepsilon_{th1})}, \quad k_{1s}^{(3)} \simeq -ic_1. \quad (47)$$

This limiting case suggests that two of the three possible $S(\varepsilon)$ poles, namely $k_{1s}^{(1,2)}$, are generated by the quark state, one pole for each k_1 branch. The third solution $k_{1s}^{(3)}$ is produced by the background \bar{P} rather than the quasi-bound quark state. In the approximation of eq. (47) it is clear because c_1 is determined only by the background part of the P -matrix. This S -matrix pole will still be present and located exactly at $-ic_1$ when there is no quasi-bound quark state at all and the P -matrix is given by only its background part: $P = \bar{P}$. We want to call to mind that if c_1 is estimated at the threshold then the solution $k_{1s}^{(3)} \simeq -ic_1$ is reliable only when $|c_1 b_0| < 1$.

For an arbitrary r it is very fruitful to consider the reduced R -matrix of the elastic scattering in the first channel defined as

$$R_1^{(red)}(\varepsilon, b) = \frac{1}{P_1^{(red)}(\varepsilon, b)} \equiv \left(ik_1 \frac{e^{2ik_1 b} S_{11}(\varepsilon) + 1}{e^{2ik_1 b} S_{11}(\varepsilon) - 1} \right)^{-1} = \frac{1}{k_1} \tan(k_1 b + \delta_1^{(elastic)}) \quad (48)$$

(*cf.* eq. (1)). In other words, $R_1^{(red)}$ is the inverse logarithmic derivative of the first channel radial wave function $\psi_1/\psi_1'|_{r=b}$, provided the incident wave is also taken in the first channel. After some algebra $R_1^{(red)}$ can be expressed in terms of the same parameters (45), making their phenomenological interpretation especially transparent:

$$R_1^{(red)} = \frac{1}{c_1} - \frac{\rho_1/2m}{\varepsilon - (\varepsilon_p + \Delta\varepsilon_p)} \quad (49)$$

Thus c_1 is responsible for the non-resonance (background) elastic scattering in the singular channel, whereas ρ_1 determines the resonance strength reduced to the first channel⁷, and $\Delta\varepsilon_p$ is naturally associated with the ‘‘hadronic’’ shift in its energy. Particularly, the resonance turns into a bound state when, and only when, $\varepsilon_p + \Delta\varepsilon_p < \varepsilon_{th1}$.

Now the classification of a near-threshold system behavior is straightforward. For example, let us look at the phase of the elastic scattering in the first, singular, channel. By the definition of $R^{(red)}$ (see eq. (48)), the phase equals

$$\delta_1^{(elastic)} = \arctan \left(k_1 R_1^{(red)} \right) - k_1 b_0 . \quad (50)$$

and it experiences rapid variations in the threshold region $|k_1 b_0| < 1$ when either of the two terms in eq. (49) is large with respect to b_0 .

First, suppose the second, resonant, term is negligible or absent so that $R_1^{(red)} \simeq 1/c_1$. Then one gets the familiar scattering length parameterization of the elastic amplitude

$$f_{11} \equiv \frac{1}{k_1 \cot \delta_1 - i k_1} = \frac{1}{-\frac{1}{\bar{a}_1} - i k_1 + O(b_0 k_1^2)} \quad (51)$$

with the scattering length

$$\bar{a}_1 = b_0 - \frac{1}{c_1} \Big|_{\varepsilon=\varepsilon_{th1}} . \quad (52)$$

If $|1/c_1| \gg b_0$, the scattering length is anomalously large, as it happens, for example, in NN scattering. In this case the amplitude has a pole at $k_1 \simeq i\frac{1}{\bar{a}_1} \simeq -ic_1$ and it is either a bound state, such as the deuteron, or a virtual state depending on the sign

⁷ From the form of eq. (49) one might conclude that $-\rho_1/2m$ is the residue of the pole in $R_1^{(red)}(\varepsilon)$. This is not correct in general because $\Delta\varepsilon_p$ may depend on energy and the actual residue is $-\rho_1^{eff}/2m = -\frac{\rho_1/2m}{(1-\frac{d\Delta\varepsilon_p}{d\varepsilon})} \Big|_{\varepsilon=\varepsilon_p+\Delta\varepsilon_p}$. This effect is especially important at a threshold where the energy dependence in $\Delta\varepsilon_p$ is strong. A similar remark applies to c_1 .

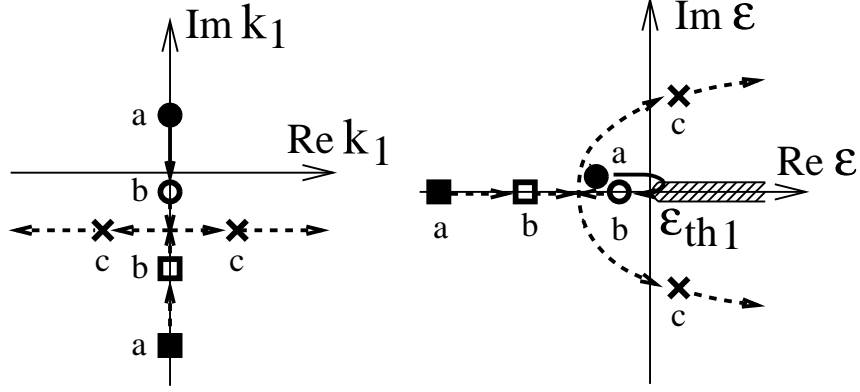


FIG. 2. The S -matrix pole dynamics for a narrow quark state with its mass increasing at the lowest threshold. The complex planes of the momentum k_1 (left) and the energy (right) are shown. Note that as the pole marked by the circle goes from the upper k_1 half-plane down to the lower half-plane, it moves from the physical energy sheet under the cut onto the unphysical sheet.

of \bar{a}_1 . Note that $O(b_0 k_1^2)$ (effective range) corrections to the amplitude in eq. (51) come from both c_1 energy dependence and the $k_1 b_0$ term in eq. (50).

Second, we consider the situation when the resonant term in $R_1^{(red)}$ has its pole near the threshold and suppose that the “background” $1/c_1$ is of the “normal” magnitude, $|1/c_1| \leq b_0$, so that $(k_1/c_1)^2$ is much less than one in the range of our interest, eq. (43). If the width, ρ_1 , is large ($\rho_1 \geq 1/b_0$), we get the same “scattering length” phenomenology with the scattering length

$$a_1 = \bar{a}_1 - \frac{\rho_1}{2m\varepsilon_1} \Big|_{\varepsilon=\varepsilon_{th1}}, \quad \varepsilon_1 \equiv \varepsilon_p + \Delta\varepsilon_p - \varepsilon_{th1} \quad (53)$$

and $O(b_0 k_1^2)$ effective range corrections, just as in eq. (51). For such a large ρ_1 the scattering amplitudes and S -matrix can have again no more than one near-threshold pole that arises when $|\frac{\rho_1}{2m\varepsilon_1}| \gg b_0$ and is located on the imaginary k_1 axis:

$$k_{1s} \simeq i \frac{1}{a_1} \simeq -i \rho_1 / 2m\varepsilon_1. \quad (54)$$

It will be a stable particle if $\varepsilon_p + \Delta\varepsilon_p < \varepsilon_{th1}$ and a virtual state if $\varepsilon_p + \Delta\varepsilon_p > \varepsilon_{th1}$. In the alternative case of a narrow resonance ($\rho_1 \ll 1/b_0$) another S -matrix pole appears. In fact, in the region $(k_1/c_1)^2 \ll 1$ the equation (44) that specifies the S pole momenta becomes quadratic:

$$\frac{k_{1s}^2}{2m^*} + i \frac{k_{1s} \rho_1}{2m} - \varepsilon_1 = 0, \quad m^* \equiv \frac{m}{1 - \frac{\rho_1}{c_1}}. \quad (55)$$

If $\rho_1 \ll 1/b_0$ then $m^* \simeq m$, for we assumed that $|1/c_1| \leq b_0$, and the solutions of eq. (55) have their average at

$$\frac{1}{2}(k_{1s}^{(1)} + k_{1s}^{(2)}) \simeq -i\frac{\rho_1}{2} . \quad (56)$$

Therefore when $\rho_1 \ll 1/b_0$ and the quark state is not far from the threshold, $|\varepsilon_1| < b_0^{-2}/2m$, both solutions get into the circle (43). The arrangement of the S poles on the momentum and energy complex planes for different values of ε_1 is shown in Fig. 2. Despite the intricate analytic structure, elastic scattering in the singular channel shows nothing more than a narrow resonance slightly distorted by the threshold (see Fig. 6 (a) for example). The scattering phase will have the form $\delta_1^{(elastic)} = \bar{\delta}_1 + \delta_1^r$ with

$$\bar{\delta}_1 = \arctan(k_1/c_1) - k_1 b_0 \simeq -\bar{a}_1 k_1 \quad (57)$$

and

$$\delta_1^r \simeq -\arctan\left(\frac{k_1 \rho_1 / 2m}{\varepsilon - \varepsilon_p - \Delta \varepsilon_p}\right), \quad (58)$$

omitting the terms $O(k_1^2/c_1^2)$ and $O(\rho_1/c_1)$. In practice, the parameterization of scattering amplitudes by the reduced R -matrix, eq. (48), is inconvenient since the parameter b_0 is not strictly defined and model dependent. The reduced K -matrix, $K_1^{(red)}(\varepsilon) \equiv R_1^{(red)}(\varepsilon, b)|_{b=0}$ is free from this deficiency and can be easily found:

$$K_1^{(red)}(\varepsilon) \simeq -\bar{a}'_1 - \frac{\rho'_1/2m}{\varepsilon - \varepsilon_{th1} - \varepsilon'_1}, \quad (59)$$

where

$$\bar{a}'_1 = \frac{\bar{a}_1}{1 - \rho_1 b_0}, \quad \rho'_1 = \rho_1 \frac{1 - \rho_1 b_0 + 2m\varepsilon_r \bar{a}_1 b_0}{(1 - \rho_1 b_0)^2}, \quad \varepsilon'_1 = \frac{\varepsilon_1}{1 - \rho_1 b_0}. \quad (60)$$

The reduced K -matrix in eq. (59) gives the correct elastic amplitude

$$f_{11} = \frac{1}{(K_1^{(red)})^{-1} - ik_1} \quad (61)$$

up to terms $O(k_1^2 b_0 c_1^{-1})$ regardless of the magnitude of ρ_1 .

We have not considered the possibility that both terms in the reduced R -matrix in eq. (49) are anomalously large. This situation may give rise to many interesting phenomena. Nevertheless, we will not discuss them here because the chance of such a double accident (large ‘‘potential’’ scattering length \bar{a}_1 and a quark state close to the threshold) should be small and we are not aware of a real two-hadron system with these properties.

So far we treated elastic amplitudes only. Inelastic S -matrix elements also present practical interest, even when the other, non-singular, channels are closed and inelastic scattering is energy forbidden. For example, if a six-quark singlet state H exists

between $\Lambda\Lambda$ and $N\Xi$ thresholds, the following production experiment is possible: $K^-d \rightarrow K^0\Xi N \rightarrow K^0H \rightarrow K^0\Lambda\Lambda$ where the intermediate Ξ is virtual. With reasonable assumptions, the amplitude of this process is proportional to $S_{\Lambda\Lambda,\Xi N}$. In general, the off-diagonal S -matrix element between the singular, first, channel and a non-singular channel l is given by the formula (31) as

$$S_{1l} = \bar{S}_{1l} - i \frac{\chi_1 \chi_l}{\varepsilon - \varepsilon_r + i \frac{\gamma}{2}} , \quad (62)$$

where the ‘‘resonance’’ energy and width are completely determined by the same three parameters $-\varepsilon_p + \Delta\varepsilon_p$, ρ_1 , and c_1 :

$$\varepsilon_r - i \frac{\gamma}{2} = \varepsilon_p + \Delta\varepsilon_p - \frac{\rho_1 c_1}{2m} \frac{(k_1/c_1)^2}{1 + (k_1/c_1)^2} - i \frac{k_1 \rho_1 / 2m}{1 + (k_1/c_1)^2} , \quad (63)$$

and so is χ_1 :

$$\chi_1 = \sqrt{k_1 \rho_1 / m} \frac{e^{-ik_1 b_0}}{1 - ik_1 / c_1} . \quad (64)$$

Near the first threshold when $k_1 \ll 1/b_0, 1/\bar{a}_1$ we have the anticipated result that $\gamma \propto k_1$, $\chi_1 \propto \sqrt{\gamma} \propto \sqrt{k_1}$, and ε_r , χ_l have finite magnitude :

$$\varepsilon_r - i \frac{\gamma}{2} = \left(\varepsilon_p + \Delta\varepsilon_p + O(k_1^2) \right) - i \frac{k_1 \rho_1 / m}{2} \left(1 + O(k_1^2) \right) , \quad (65)$$

$$\chi_1 \simeq \sqrt{k_1 \rho_1 / m} (1 - i\bar{a}_1 k_1) , \quad \chi_l = \sqrt{k_l \rho_l / m} (1 + O(ik_1)) . \quad (66)$$

In conclusion, we discuss the new features introduced to our analysis when one of the non-singular strongly coupled channels is *open*. In this case all the previous equations of this section formally remain valid, of course with the subscript ‘‘1’’ replaced by the number of the singular channel, ‘‘2’’. The first real difference comes from the fact that κ_l in the analogue of eq. (46),

$$\bar{\kappa}_l = \frac{1}{i} k_l (1 - \delta_{l2}) , \quad (67)$$

is now complex for $l=1$ giving non-vanishing imaginary part to the parameters $\Delta\varepsilon_p$, ρ_2 , and c_2 in eq. (45). As a consequence, the scattering lengths a_2 or \bar{a}_2 become complex. At the second threshold similar to eq. (65),

$$\varepsilon_r - i \frac{\gamma}{2} = \left(\varepsilon_p + \Delta\varepsilon_p + O(k_2^2) \right) - i \frac{k_2 \rho_2 / m}{2} \left(1 + O(k_2^2) \right) . \quad (68)$$

But ε_r and γ were originally defined as real quantities whereas $\Delta\varepsilon_p$ and ρ_2 in this equation are complex. Therefore the ‘‘smooth term’’, $\varepsilon_p + \Delta\varepsilon_p + O(k_2^2)$, in eq. (68)

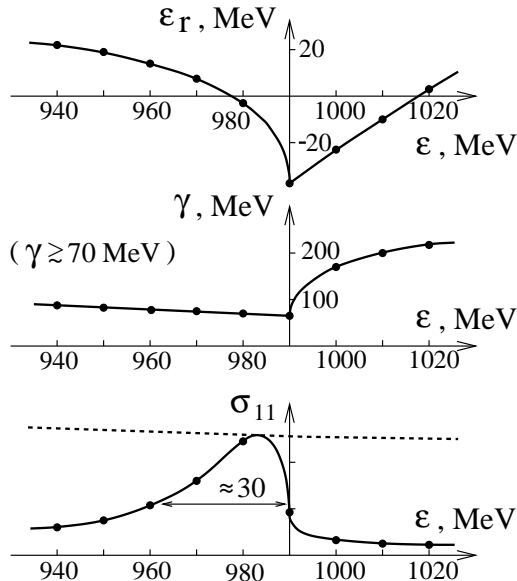


FIG. 3. The effective resonance position (ε_r), effective width (γ), and elastic cross section (σ_{11}) as functions of energy ε for a two-channel model with a P -pole close to the second threshold at 990 MeV . The dashed line on the σ_{11} plot is the unitary limit for s -wave scattering. The half-width of the peak in the cross-section is considerably less than γ .

contributes to both ε_r and γ providing a non-vanishing width just at the second threshold and below. Due to the complex ρ_2 , the “cusp term”, $ik_2\rho_2/2m$, also contributes to ε_r and to γ above and under the threshold. Nevertheless, from the definition of ρ_2 one can see that its imaginary part is suppressed by the factor b_0/k_1 , which is less than one by our earlier assumptions. That is $\gamma(\varepsilon)$ still has the bigger cusp just above the threshold and $\varepsilon_r(\varepsilon)$ just below. In Fig. 3 we present a two-channel example where two hypothetical particles with the equal masses 140 MeV in one channel and 495 MeV in the other are coupled by a primitive at 1040 MeV , which is 50 MeV above the second threshold. The couplings ξ_1 and ξ_2 are taken to be equal. Notice that in this model γ exceeds 70 MeV for all energies in the range of interest whereas the observed half-width of the corresponding resonance is as small as 30 MeV . This is the result of strong energy dependence in $\varepsilon_r(\varepsilon)$ and $\gamma(\varepsilon)$ at the threshold that has another consequence. Namely, the right slope of the resonance curve, which is closer to the threshold, is considerably more steep than the left one. The masses in this example were chosen to be those of pion and kaon that form the decay channels of the $f_0(980)$ resonance, eq. (19). Of course, this simple nonrelativistic model is not able to provide an adequate description of $f_0(980)$, but the resemblance of the cross-section in Fig. 3 to the observed $\pi\pi$ scattering is striking.

When the singular threshold is not the lowest in energy, we also have the possibility of studying the elastic scattering in the non-singular open channel. For a narrow quark state bringing two near-threshold poles to the S -matrix one can use the same formula (31) with the resonance position and width just discussed (see eq. (68) and the

text that follows it). One pole, produced by a large “background” scattering length \bar{a}_2 or a broad quark state at the threshold, may also appear as a narrow resonance in the non-singular channel. To see this, let us write down the element S_{11} in full, extracting the rapidly varying singular momentum $\kappa_2 \equiv \frac{1}{i}k_2$:

$$S_{11} = e^{-2ik_1b_0} \frac{1 + ik_1/d_1}{1 - ik_1/d_1} \frac{1 + \kappa_2/c_2^*}{1 + \kappa_2/c_2} . \quad (69)$$

We will present the expression for d_1 in a moment, and c_2 is defined as earlier in eqs.(45,46) with $1 \rightarrow 2$ but \bar{P} is now identified with P . In particular, $1/c_2$ gives the scattering length in the singular channel:

$$a_2 = b_0 - 1/c_2 . \quad (70)$$

Separating the real and imaginary parts in $1/c_2$ one obtains

$$\frac{1}{c_2} = \frac{1}{d_2} \left[1 - \alpha_{12} \frac{k_1^2}{k_1^2 + d_1^2} \right] + i \frac{\alpha_{12}}{d_2} \frac{k_1 d_1}{k_1^2 + d_1^2} . \quad (71)$$

The quantities d_1 , d_2 , and α_{12} are real and constructed from the matrix

$$D_{ij} \equiv P_{ij} + \sum_{l \neq 1,2} \delta_{il} \delta_{jl} \kappa_l \quad (i, j = 1, 2, \dots, n) \quad (72)$$

as follows:

$$\frac{1}{d_k} \equiv \left(\frac{1}{D} \right)_{kk} \quad (k = 1, 2) , \quad \alpha_{12} \equiv d_1 d_2 \left(\frac{1}{D} \right)_{12} \left(\frac{1}{D} \right)_{21} . \quad (73)$$

If for some system $Re(1/c_2)$ is negative and $Im(1/c_2)$ turns out to be small then the S-matrix element in eq. (69) has a sharp resonance when

$$\kappa_2 Re\left(\frac{1}{c_2}\right) \simeq -1 . \quad (74)$$

This effect has a natural interpretation. In fact, the small imaginary part of $1/c_2$, which by eq. (70) up to the sign equals the imaginary part of the scattering length in the second channel, means that the coupling between the first and the second channel is weak. If we turned this coupling off completely, we would find that the hadrons in the second channel form a bound state just at the energy satisfying to eq. (74), similar to the bound state at $k_{1s}^{(3)}$ in eq. (47). The small coupling of this state to the first channel gives rise to the resonance in the first channel elastic scattering exactly at the would-be-bound state energy determined by the equation (74). Presumably, this is the origin of $\Lambda(1405)$ resonance in the $\Sigma\pi$ scattering just under the $\bar{K}N$ threshold.

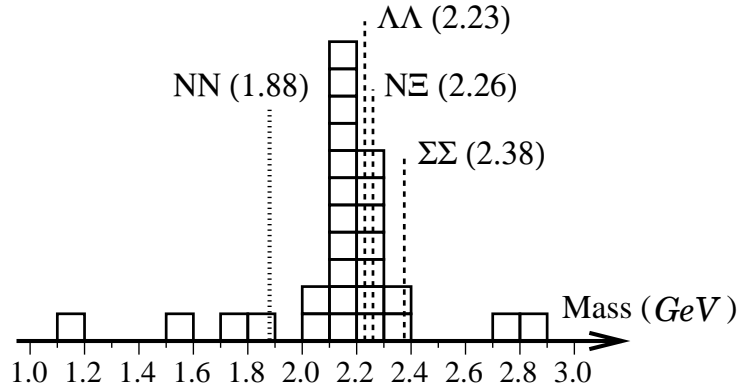


FIG. 4. The histogram showing the theoretical predictions of the H -dibaryon mass verses the energy scale and its weak – NN – and strong – $\Lambda\Lambda$, $N\Xi$, $\Sigma\Sigma$ – decay thresholds.

IV. APPLICATION TO THE H DIBARYON

The hypothetical H -dibaryon with its mass close to the $\Lambda\Lambda$ threshold was our major illustration throughout this paper. About thirty theoretical predictions of its mass have been made. As shown in Fig. 4^[8], they range from below $2M_N$, when the H would be a more stable form of hadronic matter than nuclei, to 2.8 GeV , well above its strong decay threshold into $\Lambda\Lambda$ at 2.23 GeV . So far, the experimental searches for H dibaryon have given inconclusive results⁸, although no definitive observations of double hypernuclei which would preclude a deeply bound H have not been reported either. These experiments were usually aimed at the H -particle which is stable to strong decay. However, the uncertain theoretical and experimental status of the H -dibaryon leaves much room for an H which is heavier than $2M_\Lambda$. In this case it would appear as a resonance-like structure in the two-baryon sector with $S=-2$, $I=0$, and $J=0$. Furthermore, the small projection of H onto the baryon channels, $1/5$ in the flavor $SU(3)$ limit by eq. (15), suggests that the corresponding resonance might be more or less narrow and could be detected in an experiment which is sensitive to a two-baryon scattering amplitude in the $SU(3)_f$ singlet channel. The amplitude for such a typical production experiment schematically shown on Fig. 5 a) will be of the form

$$M = \sum_{B_1 B_2} A_{B_1 B_2} T_{B_1 B_2 \rightarrow B'_1 B'_2}(s') + \overline{M} , \quad (75)$$

⁸ The two candidate events reported in Ref. [9] have recently been reanalyzed^[10] and found likely to be misidentified K_L decays.

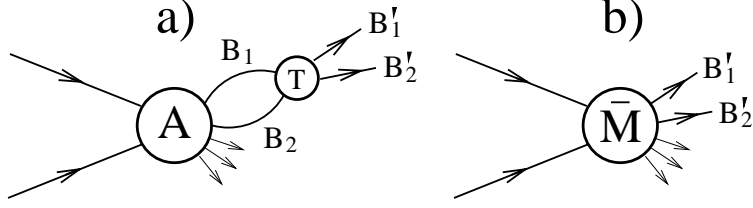


FIG. 5. (a) An inclusive two baryon production amplitude sensitive to the H -particle coupling. $B_1 B_2$ and $B'_1 B'_2$ are some of the baryon pairs from eq. (76) in the text. (b) The background amplitude for $B'_1 B'_2$ production.

where $A_{B_1 B_2}$ and \bar{M} are some smoothly varying production amplitudes and the two-baryon scattering amplitude $T_{B_1 B_2 \rightarrow B'_1 B'_2}(s')$ exhibits resonance behavior when the $B'_1 B'_2$ invariant mass $\sqrt{s'}$ is close to the mass of the H -particle. Let us remember that the flavor and the spin singlet $H=(uuddss)_{singl}$ gives rise to a pole (primitive) in the two-baryon scattering P -matrix that by eq. (18) has equal couplings, $\xi_i = \pm\sqrt{1/8}$, to the following channels

$$\Xi^- p, \Xi^0 n, p \Xi^-, n \Xi^0, \Sigma^- \Sigma^+, \Sigma^+ \Sigma^-, \Sigma^0 \Sigma^0, \Lambda \Lambda . \quad (76)$$

The two-baryon threshold energies are shown in Fig. 4. In the sections IIb, IIIa we saw that the interaction with hadrons effectively downshifts the H particle energy by the amount $\Delta\varepsilon_p$ estimated in the Appendix as

$$\Delta\varepsilon_p \sim (-40 \text{ MeV}) - (-150 \text{ MeV}) . \quad (77)$$

A deeply bound H ,

$$\varepsilon_p + \Delta\varepsilon_p < \varepsilon_{\Lambda\Lambda} - b_0^{-2}/2m \simeq 2210 \text{ MeV} \quad (78)$$

obviously would not affect the baryon scattering. If it is unbound and far from hadronic thresholds,

$$\left| \varepsilon_p + \Delta\varepsilon_p - \varepsilon_{\Lambda\Lambda/N\Xi/\Sigma\Sigma} \right| > b_0^{-2}/2m \simeq 20 \text{ MeV} , \quad (79)$$

and the residue r given by eq. (23) is sufficiently small, the H should appear as a typical resonance (31) in baryon-baryon scattering that has comparable couplings χ_i , eq. (33), to all of the channels (76) which are open at the resonance energy. However, whether the H -resonance should be narrow is an open question. Let us characterize the H width by $\Delta E_H \equiv b_0^{-1} \rho_{\Lambda\Lambda}/2m$ that is the energy interval where the resonant term in eq. (49) is important for $\Lambda\Lambda$ scattering. Then our estimates in the Appendix give that ΔE_H may range from 10 MeV to 40 MeV. Unknown nonperturbative dynamics may also change the situation significantly, and the resonance can be so broad that the two-baryon quasielastic amplitudes will not show any apparent peaks. In this case the reduced R -matrix defined by eq. (48) in terms of the measurable elastic scattering

phase will still have a pole as given by eq. (49). Therefore, the H -primitive can be experimentally *observed* even if there is no actual particle associated with it.

Now we consider what happens if the H is close to one of the thresholds in eq. (76). Suppose it is the lowest threshold, $\Lambda\Lambda$. There is no particular reason to expect anomalously large potential scattering in this channel ^[11]. If the pole in $R_{\Lambda\Lambda}^{(red)}$ is narrow, the elastic $\Lambda\Lambda$ scattering amplitude and phase will have the classical Breit-Wigner forms with the width proportional to the $\Lambda\Lambda$ relative momentum, eq. (58), and the inelastic (quasielastic) scattering will be given by eqs.(62–66). All these quantities can be expressed in terms of the three real parameters $(\varepsilon_p + \Delta\varepsilon_p)$, $\rho_{\Lambda\Lambda}$, and \bar{a}_1 for elastic scattering and the additional parameter $\rho_{N\Xi(\Sigma\Sigma)}$ for transition to or from another channel. Close to the $\Lambda\Lambda$ threshold $R_{\Lambda\Lambda}^{(red)}$ approaches the reduced K -matrix of the elastic $\Lambda\Lambda$ scattering and one should find a narrow pole in the latter as well. If the couplings $\rho_{\Lambda\Lambda/N\Xi/\Sigma\Sigma}$ and the residues of the $R_{\Lambda\Lambda}^{(red)}$ or $K_{\Lambda\Lambda}^{(red)}$ poles are not small, the $\Lambda\Lambda$ scattering will be well described by the scattering length in eq. (53) with no dramatic resonance effects, but this length and the cross-section may be anomalously large when the corresponding pole in the S -matrix, eq. (54), is close to the $\Lambda\Lambda$ threshold. In many aspects this very last possibility will resemble a quasi-bound two- Λ state. The characteristic plots of the amplitudes for the cases above are presented in Fig. 6.

Our formalism does not make specific predictions for background (potential) scattering parameterized by \bar{P} . One should expect that $\bar{P}(\varepsilon)$ has no poles in the region of interest. These poles might come from the excited H states and from other, non-singlet, flavor representations of the six-quark system. One-quark excitation energy is of the order of $\pi/b_0 \sim 500 \text{ MeV}$. As the Table I of the Ref. [5] shows, the other six-quark flavor multiplets have their ground states at the energies at least 200 MeV higher than the flavor singlet mass because of color-magnetic interaction. Therefore, the matrix \bar{P} in eq. (6) should be a smooth function of energy in a broad interval $\sim 100 \text{ MeV}$ around the singlet pole. Let us briefly discuss some suggested or ongoing experiments which might be sensitive to an unbound or resonant H .

Nucleon-Nucleus collisions: The production of strange particles is plentiful when a nucleus is struck by a nucleon or another nucleus. This has been exploited in the search for the stable H -particle in the experiments E888 and E896 at the AGS. However, the same abundance of Λ 's or Ξ 's will present a problem for a detection of the H -resonance because only a small fraction of $\Lambda\Lambda$ or $N\Xi$ pairs will be produced close enough in space and with their relative momenta small enough to interact via H -formation. We estimate this fraction from the $\Lambda\Lambda$ and $N\Xi$ coalescence rate computed in Ref. [12]. That gives the order of 10^{-3} , making it very hard to see a resonant H above the background uncorrelated $\Lambda\Lambda$ or $N\Xi$ pairs.

Elastic Secondary Scattering: One can produce two Λ 's or another baryon pair in eq. (76) and hope to extract their elastic scattering amplitude from interaction in the final state, Fig. 5 a) with $B_1 B_2 = B'_1 B'_2$. The total amplitude will have the form in eq. (75) where \bar{M} will be in general large due to “direct” $\Lambda\Lambda$ production, Fig. 5 b).

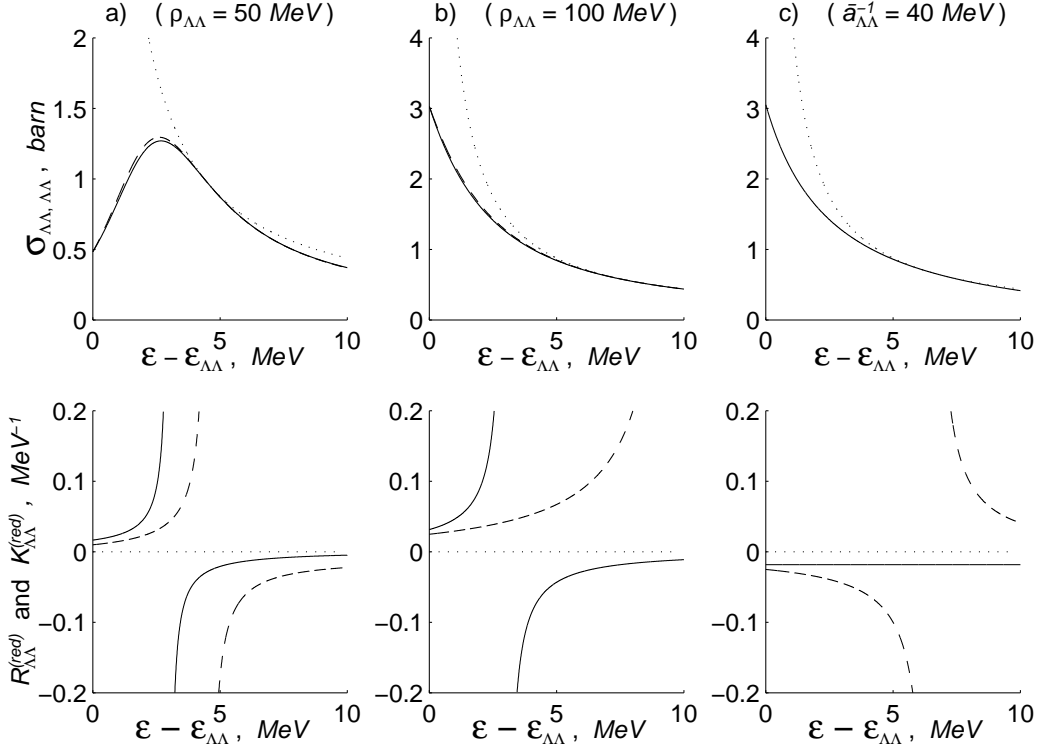


FIG. 6. The cross-section of the s -wave $\Lambda\Lambda$ elastic scattering (top) and the corresponding reduced R (bottom, solid) and K (bottom, dashed) matrices when the effective H -particle mass is close to the $\Lambda\Lambda$ threshold at $\varepsilon_{\Lambda\Lambda} = 2230 \text{ MeV}$: $\varepsilon_p + \Delta\varepsilon_p = \varepsilon_{\Lambda\Lambda} + 3 \text{ MeV}$. In the first two cases the parameter $a_{\Lambda\Lambda}^{-1}$ that characterizes the potential scattering has a “normal” magnitude 200 MeV and the width parameter $\rho_{\Lambda\Lambda}$ is 50 MeV and 100 MeV for the plots (a) and (b) correspondingly. In the case (c) the reduced R -matrix does not have a pole: $R_{\Lambda\Lambda}^{(red)} = c_{\Lambda\Lambda}^{-1} = \text{const}$ but it is anomalously large with the scattering length $\bar{a}_{\Lambda\Lambda} = (40 \text{ MeV})^{-1}$. The corresponding cross-section is almost indistinguishable with the case (b). The dashed line on the top figures (a) and (b) gives the cross-section calculated from eqs. (59) and (60). The dotted line shows the unitary limit, $4\pi/k^2$.

Quasi-Elastic Secondary Scattering: We can also suppress the diagrams like the one in Fig. 5 b) by producing, *e.g.*, a virtual or real $N\Xi$ pair and then observing it scattering into $\Lambda\Lambda$. The reactions of this kind were considered by Aerts and Dover ^[11] in connection with the stable H production. For example, take the process $K^-d \rightarrow K^0\Lambda\Lambda$. The diagrams that we are interested in are shown in Fig. 7 a). When K^- and K^0 interact with different nucleons as in Fig. 7 b), the final Λ 's can be put on the mass shell only by some additional momentum exchange between them that suppresses the corresponding amplitude and essentially makes it higher order. In that order we also have soft meson exchange, *e.g.* Fig. 7 c). The cross-section for that was estimated in Ref. [13] as $\sigma_{(N\Xi \rightarrow \Lambda\Lambda)} v_{N\Xi} \simeq 10 \text{ mb}$ at the $N\Xi$ threshold. If we take

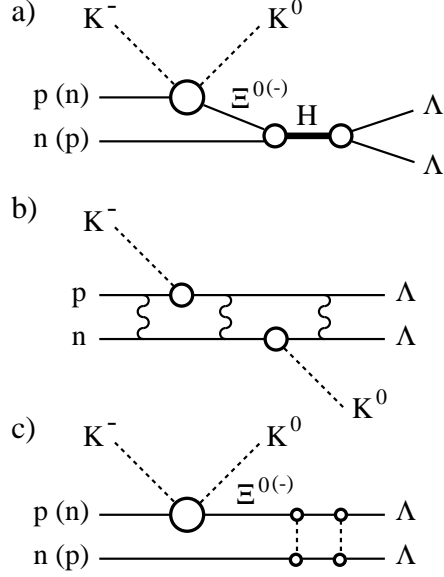


FIG. 7. (a) The lowest-order processes in $K^-d \rightarrow K^0\Lambda\Lambda$ which are sensitive to an H -resonance. (b, c) The lowest-order background to this reaction.

$\left[\left(\frac{1}{P+\bar{k}}\right)\xi\right]_{\Lambda\Lambda} \simeq \left[\left(\frac{1}{P+\bar{k}}\right)\xi\right]_{N\Xi}$, the formula (62) gives at the resonance peak, $\varepsilon=\varepsilon_r \simeq \varepsilon_{N\Xi}$, that $\sigma_{(N\Xi \rightarrow \Lambda\Lambda)}v_{N\Xi} \simeq 60 \text{ mb}$. Thus the background $\Lambda\Lambda$ production in this process may be comparable but does not exceed the resonance production as it did in the previous cases. The reactions of this form may prove most promising for a search for a resonance H above $\Lambda\Lambda$ threshold.

V. ACKNOWLEDGMENTS

The authors would like to thank B. Kerbikov and J. Engelage for stimulating discussions and useful references.

APPENDIX

The hadronic shift and width for the H -particle

In the sections IIb, IIIa we saw that the interaction with hadrons effectively shifts the H -particle energy by $\Delta\varepsilon_p$ given in eq. (45). We estimate this quantity and the other parameters, $\rho_{\Lambda\Lambda}$ and $c_{\Lambda\Lambda}$, in eq. (45) for the H -particle at the $\Lambda\Lambda$ threshold. Altogether they compose the reduced R -matrix in the $\Lambda\Lambda$ channel (eqs. (48-49)) :

$$R_{\Lambda\Lambda}^{(red)} \equiv \frac{1}{k_{\Lambda\Lambda}} \tan(k_{\Lambda\Lambda}b_0 + \delta_{\Lambda\Lambda}^{(elastic)}) = \frac{1}{c_{\Lambda\Lambda}} - \frac{\rho_{\Lambda\Lambda}/2m}{\varepsilon - (\varepsilon_p + \Delta\varepsilon_p)}. \quad (80)$$

Let us notice that if Λ -particles did not interact with each other, the P -matrix would have the lowest pole at $\varepsilon_p = 2M_\Lambda + \frac{(\pi/b_0)^2}{2m}$ with the residue

$$r_0 = -\frac{\partial \varepsilon_p}{\partial b} = -\frac{\partial}{\partial b} \left(\frac{(\pi/b)^2}{2m} \right) = \frac{\pi^2}{mb_0^3}. \quad (81)$$

For interacting Λ 's one could expect that the residue r is suppressed with respect to r_0 by the factor $\lambda = \frac{1}{5}$ due to the small projection of H onto the baryon channels (see eq. (23)). On the other hand, if r is computed in the bag-model then eq. (23) and the virial theorem [2] give

$$r_{bag \text{ mod.}} = \lambda \left. \frac{\partial \varepsilon_n}{\partial R} \frac{\partial R}{\partial b} \right|_{R=R_0} = \lambda \frac{3}{4} \frac{M_H}{R} \left. \frac{\partial R}{\partial b} \right|_{R=R_0} \simeq \lambda \frac{3}{4} \frac{M_H}{b_0}. \quad (82)$$

Taking for M_H the threshold energy $2M_\Lambda$ and accepting that $b_0 \simeq R_0 \simeq 5M_H^{1/3} \text{ GeV}^{-1} \simeq (150 \text{ MeV})^{-1}$, the ratio $\lambda r_0 / r_{bag \text{ m.}}$ is 1 : 4. This discrepancy is easily understandable. In fact, in eq. (81) the pressure on the cavity walls that determines r is exerted by heavy hadrons with the kinetic energy $(\pi/b_0)^2/2m \ll M_H$ whereas in eq. (82) we have ultra-relativistic quarks and the pressure it is proportional to their total energy $\varepsilon_{tot} \sim M_H$.

Assuming for simplicity that $\bar{P}_{ij} \sim \delta_{ij} b_0^{-1} \sim \delta_{ij} \cdot 150 \text{ (MeV)}$, we find that at the $\Lambda\Lambda$ threshold

$$\rho_{\Lambda\Lambda} \sim 300 \text{ MeV} \quad , \quad \Delta\varepsilon_p \sim -150 \text{ MeV} \quad (83)$$

if we use the bag model prediction for r in eq. (82), or

$$\rho_{\Lambda\Lambda} \sim 70 \text{ MeV} \quad , \quad \Delta\varepsilon_p \sim -40 \text{ MeV} \quad (84)$$

if r is taken as λr_0 . The contribution of the $\Lambda\Lambda$ channel, for which $\bar{\kappa}$ in eq. (45) is zero, to $\Delta\varepsilon_p$ is comparable with the $N\Xi$ channels ($p\Xi^-$, $n\Xi^0$, Ξ^-p , $n\Xi^0$) and the $\Sigma\Sigma$ channels give only 20% to the total. The actual values of the parameters $\rho_{\Lambda\Lambda}$ and $\Delta\varepsilon_p$ are probably somewhere in between the numbers in eqs. (83) and (84). Also notice that as described in the footnote on p. 15, the energy dependence in $\Delta\varepsilon_p$ may effectively change $\rho_{\Lambda\Lambda}$. For comparison, the hadronic shift computed by Badalyan and Simonov [14] was found to be 15 – 30 MeV but they included only coupling to the $\Lambda\Lambda$ channel, and larger values 150 – 200 MeV were obtained by B. Kerbikov [15] and 100 MeV by M. Soldate [3].

REFERENCES

- [1] For an elementary introduction see R. Levi Setti and T. Lasinski, *Strongly Interacting Particles* (The University of Chicago Press, Chicago and London, 1973).
- [2] R. L. Jaffe and F. E. Low, *Phys. Rev. D* **19** (1979) 2105.
- [3] M. Soldate, unpublished (1980).
- [4] Yu. A. Simonov, *Sov. J. Nucl. Phys* **36** (1982) 422.
- [5] R. L. Jaffe, *Phys. Rev. Lett.* **38** (1977) 195.
- [6] R. P. Bickerstaff and B. G. Wybourne, *J. Phys.* **G7** (1981) 275.
- [7] M. R. Pennington, in *Plots, Quarks and Strange Particles*, Proc. of the Dalitz Conference (World Scientific, 1990) p. 66.
- [8] J. R. Klein, Ph.D thesis, Princeton HEP/94/09, Princeton University (1994), thanks to P. T. Jensen and BNL E896 collaboration for pointing out this reference.
- [9] J. Belz *et al.*, *Phys. Rev. Lett.* **76** (1996) 3277.
- [10] A. Schwartz, E888 memos, **KL-497** (1996); **KL-498** (1997).
- [11] A. T. M. Aerts and C. B. Dover, *Phys. Rev. D* **28** (1983) 450.
- [12] B. A. Cole, M. Moulson, W. A. Zajc, *Phys. Lett. B* **350** (1995) 147.
- [13] M. M. Nagels, T. A. Rijken, J. J. de Swart, *Phys. Rev. D* **15** (1977) 2547; **20** (1979) 1633.
- [14] A. M. Badalyan and Yu. A. Simonov, in *Proc. of the International Conference on Hypernuclear and Kaon Physics, Heidelberg, Germany 1982*, p. 281 (Max-Planck-Institut für Kernphysik, Heidelberg, 1982).
- [15] B. Kerbikov, *Sov. J. Nucl. Phys* **39** (1984) 516.